Energy transfer, pre-reactive complex formation and recombination reactions during the collision of peroxy radicals. Electronic Supplementary Information (ESI)

Christopher David Daub,[a] Itai Zakai,[b], Rashid Valiev,[ac],
Vili-Taneli Salo,[a], R. Benny Gerber,[bd] and Theo Kurtén[a]

March 11, 2022

S1 Energetics of two peroxy radicals – comparison of different methodologies

S1.1 Stationary points

It is important to benchmark our methods by establishing the energetics of the peroxy radical complexes, and compare the different methodologies. In Tables S1 and S2 we list all of these results for the methyl peroxy, as well as the available results for other peroxy radicals of interest.

The most reliable single-reference calculation data we have available is done at the CCSD(T)-F12 level. This serves to benchmark the energies for states amenable to a single-reference description, and it can be directly expressed as a binding energy relative to the energy of the two separate radicals. However, it cannot be used to describe transition states or the pre-reactive complex since they both have significant multi-reference character in the *ab initio* treatments.

Multi-reference methods such as CASSCF and XMC-QDPT2 must therefore be used to describe the pre-reactive complex and the transition region. Because there is no reliable way to express these energies relative to the separated radicals, instead these energies are given relative to the tetroxide minimum (RO_4R) computed with CCSD(T)-F12. To clarify that these energies have a different reference state they are listed separately in Table S2.

Of particular relevance are the energy minima in the pre-reactive complex. The single-reference restricted Hartree-Fock (RHF) singlet wavefunctions are unable to correctly describe the state of two separate radicals. Since we want to study collisions of two radicals we therefore have chosen to use unrestricted Hartree-Fock (UHF) methods on both the singlet and triplet surface for all single-reference ODMx semi-empirical molecular dynamics calculations.

We can see that a unique feature of the CASSCF and XMC-QDPT2 data is that the energies of the pre-reactive complex and the tetroxide are within only a few kcal/mol, with a small barrier between them. By contrast, both semi-empirical ODM2 and ODM3 based treatments, as well as the empirical OPLS-AA force field, find that the pre-reactive complex is only weakly bound by a few kcal/mol, with the tetroxide having considerably lower energy.

Comparison of ODM2 and ODM3 methods shows that there are advantages to each.

[0a] *Department of Chemistry, University of Helsinki, P.O. Box 55, Helsinki 00014, Finland.*

[0b] *Department of Chemistry, Hebrew University of Jerusalem, Jerusalem, Israel.*

[0c] *Tomsk State University, Tomsk 634050, Russia*

[0d] *Department of Chemistry, University of California, Irvine, Irvine, CA 92697, USA.*

Method	PR	TS1	RO_4R	$2\ RO\cdot + {}^3O_2$
	methyl peroxy			
OPLS-AA	-3.74	–	–	–
ODM2, singlet	–	–	-27.22	–
ODM2+CI(14,12), singlet	-6.09	-2.92	-36.03	–
ODM2, UHF singlet	-4.02	-2.95	-27.22	–
ODM2+CI(14,12), ROHF singlet	-5.41	-3.47	-35.28	–
ODM2, triplet	-3.61	–	–	–
ODM2+CI(14,12), ROHF triplet	-3.89	–	–	–
ODM3, singlet	–	–	-12.29	–
ODM3+CI(14,12), singlet	-3.47	-1.22	-19.43	–
ODM3, UHF singlet	-3.28	1.82	-12.29	–
ODM3+CI(14,12), ROHF singlet	-3.30	-2.34	-18.12	–
ODM3, triplet	-3.28	–	–	–
ODM3+CI(14,12), ROHF triplet	-3.33	–	–	–
CCSD(T)-F12	–	–	-16.19	7.07
	acetonyl peroxy			
OPLS-AA	-6.97	–	–	
ODM2, singlet	–	–	-32.43	
ODM2, triplet	-10.30	-8.0	–	
ODM3, singlet	–	–	-16.25	
ODM3, triplet	-11.62	-2.62	–	
CCSD(T)-F12	–	–	-17.94	4.77
	t-butyl peroxy			
OPLS-AA	-4.54	–	–	
ODM2, singlet	–	–	-24.19	
ODM2, triplet	-5.34	-2.43	–	
ODM3, singlet	–	–	-8.73	
ODM3, triplet	-5.00	2.45	–	

Table S1: Potential energy for the interaction of two peroxy radicals in various states in kcal/mol. All energies are relative to the energy of two peroxy radicals at infinite separation. PR denotes the minimum energy of the pre-reactive complex, with TS1 being the energy of the transition state from PR to the the tetroxide RO_4R. Unless otherwise noted, in the SCF calculation we use restricted Hartree-Fock (RHF) for the singlet state and unrestricted Hartree-Fock (UHF) for the triplet state. ROHF denotes the use of the half-electron restricted open-shell method for MRCI calculations implemented in the MNDO code (Dral *et al.* (2019)).

While ODM3 predicts the tetroxide minimum in good agreement with CCSD(T)-F12, it also shows a somewhat high barrier (~ 5 kcal/mol) for tetroxide formation. Although ODM2 predicts the tetroxide minimum energy to be considerably lower than CCSD(T)-F12, it also features a low barrier in good agreement with the high level results. For this reason we have chosen to use ODM2 for all of our semi-empirical molecular dynamics simulations.

For a graphical comparison of the energetics of the methyl peroxy system using all of the methods employed in our study, Figure S1 shows the energies of stationary points obtained by optimizations, plotted against r_{OO}, the distance between terminal oxygens in the two radicals. Some particular XMC-QDPT2 optimized configurations of interest are also shown.

Method	PR	TS1	RO_4R	2 RO· + $^3O_2$
	methyl peroxy			
CASSCF(10,8)/6-311++G(d,p)	-1.27	1.40	0	-19.15
XMC-QDPT2(10,8)/6-311++G(d,p)	6.12	7.55	0	–
	t-butyl peroxy			
CASSCF(10,8)/6-311++G(d,p)	-4.95	7.64	0	-21.41

Table S2: Potential energy for the interaction of two peroxy radicals in various states in kcal/mol, computed by CASSCF and XMC-QDPT2 methods. The geometries of the stationary points were optimised with both methods. The energies are relative to the tetroxide (RO_4R) minimum. PR denotes the minimum energy of the pre-reactive complex, with TS1 being the energy of the transition state from PR to the the tetroxide RO_4R. All CASSCF and XMC-QDPT2 data are from Valiev *et al.* (2019).

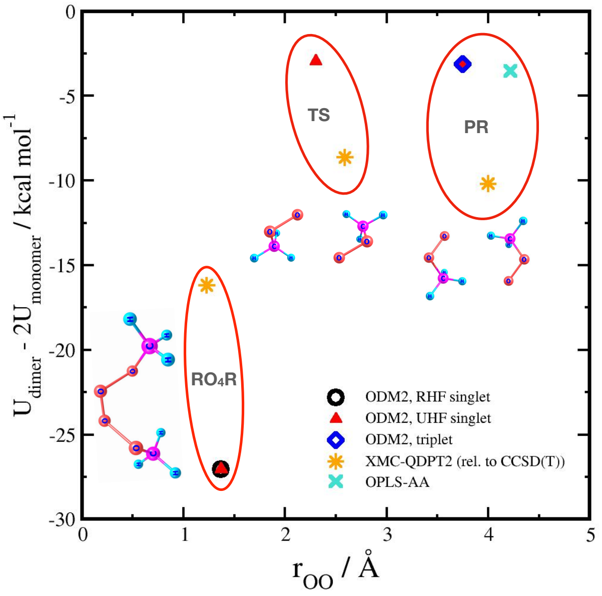

Figure S1: Stationary points (PR = pre-reactive complex, TS = transition state, RO_4R = tetroxide) on the potential energy surface of two methyl peroxy radicals as a function of the distance between the terminal oxygen atoms, r_{OO}, using all of the methods highlighted in this study. The energy is shown relative to the energy of two radicals at infinite separation (twice the energy of an isolated doublet radical in the case of the RHF singlet). XMC-QDPT2 energies are shown with the energy of the RO_4R minimum set equal to that of the CCSD(T)-F12 value shown in Table S1. Snapshots were computed with XMC-QDPT2 and taken from Valiev *et al.* (2019).

S1.2 Constrained optimizations – the influence of MRCI on the ODM2 potential surface

In Figure S2, we show the impact of including multi-reference configuration interaction (MRCI) in the semi-empirical calculations using ODM2. These curves were obtained by holding r_{OO} constant while the rest of the molecular geometry was optimized to find the energy minimum.

We focus on the calculations without configuration interaction first. As we have

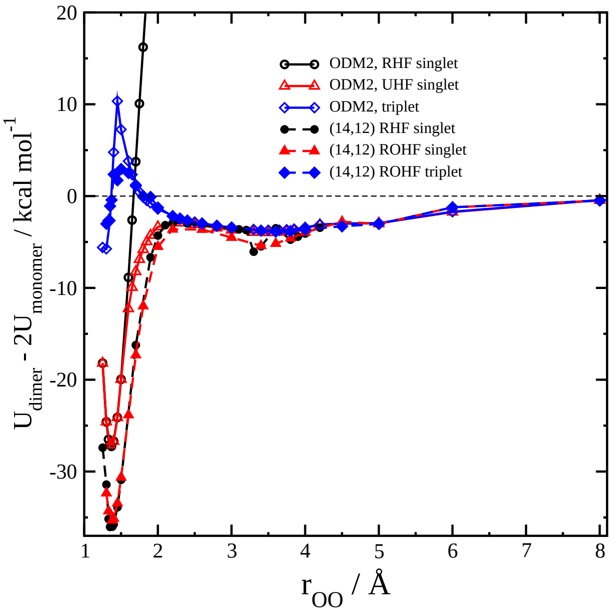

Figure S2: Comparison of the potential energy of two methyl peroxy radicals as a function of the distance between the terminal oxygen atoms, r_{OO}, showing the impact of including multi-reference configuration interaction (MRCI) in semi-empirical calculations using ODM2. The energy is shown relative to the energy of two radicals at infinite separation. Open-shell calculations with MRCI implement the half-electron ROHF method.

already seen from the CCSD(T)-F12 data, constrained optimizations using standard restricted Hartree-Fock (RHF) wavefunctions on the singlet surface work well to describe the tetroxide intermediate state (RO_4R). As mentioned above, as r_{OO} is increased, the RHF singlet is no longer an accurate description of two separate peroxy radicals. A very high barrier finally gives way when $r_{OO} \gtrsim 2.2$ Å to optimized geometries in which a hydrogen atom has shifted to form $CH_2OO + CH_3OOH$ (not shown).

It is possible to describe the combination of the doublet ground states for each peroxide radical as an overall triplet. As such, we see that the optimizations in the triplet state predict a shallow minimum with $r_{OO} \sim 3.5$ Å. The geometry of this minimum is similar to that of the optimized pre-reactive complex seen in higher level calculations. However, the depth of the minimum in comparison with the RO_4R state is much shallower. The binding energy of the pre-reactive complex is close to that obtained with the OPLS-AA force field, suggesting that this small binding energy is mainly due to weak Van der Waals and electrostatic forces. As r_{OO} lowers below ~ 1.5 Å, the triplet state optimizations end up in $CH_3O + CH_3O_3$ configurations.

The only single configuration and single reference semi-empirical surface which can describe the range of relevant r_{OO} values from the tetroxide to the separated radicals is an open-shell, unrestricted Hartree-Fock (UHF) calculation. On the one hand, ODM2 UHF calculations have a low barrier from the pre-reactive complex to the tetroxide, in agreement with the CASSCF and XMC-QDPT2 results. However the ODM2 tetroxide minimum energy is much lower than the CCSD(T)-F12 result. Since in this study we focus on tetroxide formation, we chose to use ODM2 over ODM3.

Incorporating MRCI in the ODM2 calculations has several important effects. Most strikingly, including the influence of additional excited states allows the RHF calculation in the singlet state to qualitatively correctly describe the transition state as well as the prereactive complex, although it still fails to converge for values of $r_{OO} \gtrsim 4.5$ Å. With ODM2 MRCI does not change the barrier height much, but it does change the barrier location to higher values of r_{OO}. It is also worth noting that MRCI lowers the tetroxide minimum energy significantly.

S2 $T_1 \rightarrow S_0$ transitions with varying distance criterion

The distance criterion for the $T_1 \rightarrow S_0$ transitions in our model presented in section 2.2.2 of the main article was set to be $r_{OO} < 2.5$ Å. This criterion was determined based on the calculations presented by Minaev and Yashchuk (2003) that predict a sufficiently large spin-orbit coupling between singlet to triplet for molecular oxygen at r_{OO} distances of less than 2.5 Å. We investigated how the transition probability varies with varying r_{OO} distances, and the results of this investigation are presented in Figure S3. It can be seen that below 2.0 Å no transitions occur (*i.e.* r_{OO} is never less than 2.0 Å during the simulation), while the probability for $T_1 \rightarrow S_0$ transitions increases sharply from 2.5 Å and up to 3.0 Å. We note, however, that these results did not guide our choice in the $r_{OO} < 2.5$ Å criterion, as it was determined solely based on the calculated spin-orbit coupling by Minaev and Yashchuk (2003).

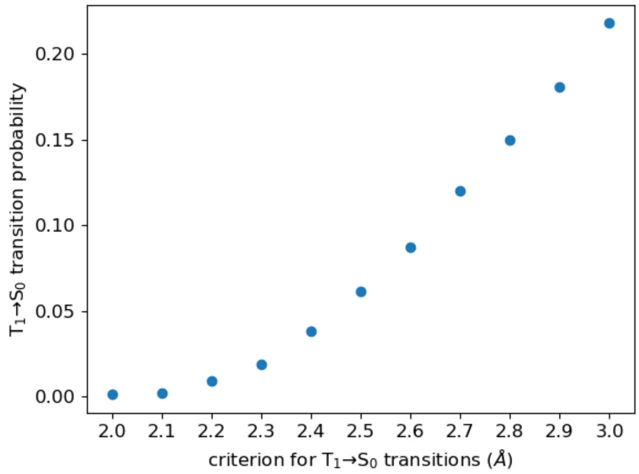

Figure S3: Probability of $T_1 \rightarrow S_0$ transitions as a function of r_{OO}.

S3 Energetics of molecular dynamics trajectories

It is also worth examining some examples of the molecular dynamics (MD) trajectories computed using different methods. Figure S4 shows the potential energy during a collision between methyl peroxy radicals, begun on the T_1 surface and transitioning to the S_0 surface. Figure S5 compares the potential energy calculated as a function of r_{OO} during the initial formation steps of the tetroxide intermediate, calculated using both ODM2 and XMC-QDPT methods.

All of the ODM2 MD trajectories on T_1 and S_0 were computed using an unrestricted Hartree-Fock (UHF) method.

We used ODM2 to simulate collisions between the radicals while, on the other hand, XMC-QDPT2 trajectories started from the optimized minimum pre-reactive complex geometry. However, a comparison of the energetics in the r_{OO} distances that were sampled by the molecular dynamics simulations of both methods (2.5 Å$< r_{OO} <$ 4.0 Å) reveals a shallow decrease in potential energy with decreasing r_{OO} which is common to both methods. This validates the ODM2 potential.

Since the barrier between the equilibrium geometry and the tetroxide is very low, the additional kinetic energy at T = 300 K is sufficient to drive the formation of the tetroxide in the XMC-QDPT2 trajectories.

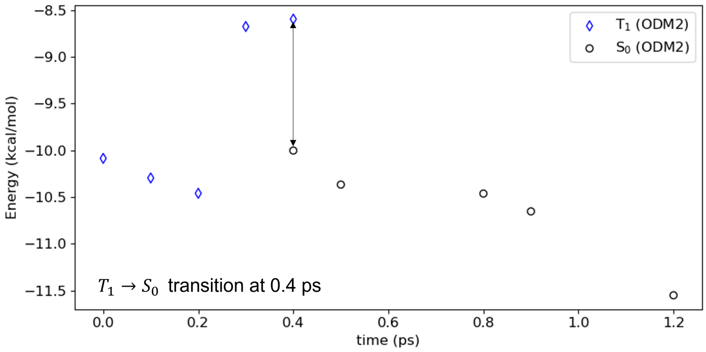

Figure S4: The potential energy during a collision trajectory of methyl peroxy radicals that starts on the T_1 potential (blue) and undergoes a transition to S_0 (black) once the distance-based criterion ($r_{OO} <$ 2.5 Å) is satisfied.

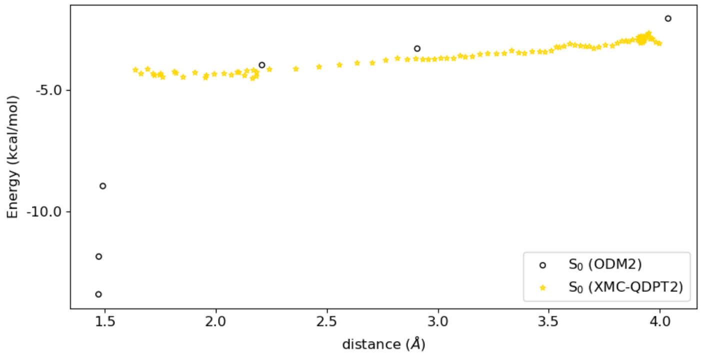

Figure S5: The potential energy as a function of the distance between the radical oxygen atoms: (Black) The potential energy at several time steps taken from a trajectory using the S_0 surface of ODM2 (Yellow) The average potential during simulations with the XMC-QDPT2 potential. We stress that the XMC-QDPT2 trajectories started from the optimized pre-reactive complex, while the ODM2 trajectory started from a non-equilibrium state.

S4 Description of trajectory movies

- **cas.mp4**: Movie of tetroxide (RO_4R) formation calculated using the XMC-QDPT2 method. The total trajectory length is 1 ps.
- **odm2_tet.mp4**: Movie of RO_4R formation calculated using the ODM2 method. The total trajectory length is 5 ps.
- **opls.mp4**: Movie of unreactive collision showing long-lived complex formation calculated using the OPLS-AA method. The total trajectory length is 40 ps.

S5 Comparison of computational costs of different methods

Method	# of CPU's	t_c
OPLS-AA/LAMMPS	1	6.3 μs
ODM2/MNDO	1	12.1 ms
XMC-QDPT2/Firefly	24	$\sim$ 180 s

Table S3: The computational costs of all of the methods we used. All data is from MD simulations of two methyl peroxy radicals. t_c is the computing time per simulation timestep. All LAMMPS simulations and all Firefly simulations were run on Xeon Gold 6230 CPU's with a clock speed of 2.1 GHz.

References

P. O. Dral, X. Wu and W. Thiel, *J. Chem. Theory Comput.*, 2019, **15**, 1743–1760.

R. R. Valiev, G. Hasan, V.-T. Salo, J. Kubečka and T. Kurtén, *J. Phys. Chem. A*, 2019, **123**, 6596–6604.

B. F. Minaev and L. B. Yashchuk, *Opt. Spectrosc.*, 2003, **95**, 553–559.